

Data/moment-driven approaches for fast predictive control of collective dynamics

Giacomo Albi¹, Sara Bicego², Michael Herty³, Yuyang Huang², Dante Kalise², and Chiara Segala³

¹ Albi Dipartimento di Informatica, Università di Verona, Verona, Italy.
 e-mail: s.giacomo.albi@univr.it

²Department of Mathematics, Imperial College London, United Kingdom.
 e-mail: s.bicego21, yuyang.huang21, dkaliseb@imperial.ac.uk

³IGPM, RWTH Aachen University, Templergraben 55, D-52062 Aachen, Germany.
 e-mail: herty, segala@igpm.rwth-aachen.de

February 27, 2024

Abstract

Feedback control synthesis for large-scale particle systems is reviewed in the framework of model predictive control (MPC). The high-dimensional character of collective dynamics hampers the performance of traditional MPC algorithms based on fast online dynamic optimization at every time step. Two alternatives to MPC are proposed. First, the use of supervised learning techniques for the offline approximation of optimal feedback laws is discussed. Then, a procedure based on sequential linearization of the dynamics based on macroscopic quantities of the particle ensemble is reviewed. Both approaches circumvent the online solution of optimal control problems enabling fast, real-time, feedback synthesis for large-scale particle systems. Numerical experiments assess the performance of the proposed algorithms.

1 Introduction

The description of collective phenomena by means of agent-based systems is a consolidate line of research in several scientific fields such as socio-economics, biology, and robotics, as highlighted in [1, 17, 30, 35, 53, 51, 41, 59]. The mathematical modeling of agent-based systems consists with a large ensemble of differential equations describing the evolution of the trajectories of N particles, whose dynamics is ruled by the superposition of binary interaction forces. These interactions encode nonlinear mechanisms based on different social principles like attraction, repulsion, and alignment. One distinctive aspect of these models lies in their capability of reproducing intricate dynamics such as self-organized patterns, including consensus, flocking, and milling, as discussed in [46, 77, 33, 39, 69].

A question of particular interest pertains to determining external control actions capable of influencing the collective behavior of these systems, which can be properly formulated as an optimal control problem. This understanding is crucial for various practical applications, facilitating the development of tailored strategies such as collision-avoidance protocols for swarm robotics [28, 71, 72, 44], pedestrian evacuation strategies for crowd

M.H. and C.S. thank the Deutsche Forschungsgemeinschaft (DFG, German Research Foundation) for the financial support 442047500/SFB1481 within the projects B04, B05, B06, and SPP 2298 Theoretical Foundations of Deep Learning within the Project(s) HE5386/23-1, Meanfield Theorie zur Analysis von Deep Learning Methoden (462234017). G.A. is member of GNCS of INdAM, and thanks the support of MIUR-PRIN Project 2022 PNRR No. P2022JC95T, Data-driven discovery and control of multi-scale interacting artificial agent systems. This research was supported by the UK Engineering and Physical Sciences Research Council (EPSRC) grant EP/T024429/1

dynamics [4, 32, 38, 21], interventions assessment in traffic management [78, 49, 75], and learning of opinion dynamics [5, 8, 45]. However, the high dimensionality given by the state space and the large number of agents does not usually allow the synthesis of optimal feedback control by means of direct methods, see for example [24, 13]. Hence, the development of novel efficient algorithms are key to handling real-time applications, which often stumble upon cumbersome software and hardware requirements.

Our aim is to approach this task from various perspectives by reviewing techniques developed in the context of Model Predictive Control (MPC) methods for approximating control strategies for agent-based systems. One of the key challenges associated with MPC strategies is its computational complexity, given the need for subsequent solutions to several optimal control problems. This can be computationally intensive, especially for high-dimensional systems and long prediction horizons.

The research community has been introducing promising remedies for these problems, involving the simplification of either the predictive models or the optimization problems, to reduce the computational complexity while maintaining acceptable control performance. Among the various proposed methodologies, we cite Reduced-Order MPC [80, 56, 48], linearization techniques [19], lookup tables (e.g. explicit MPC [9, 18]), fast-update schemes [79], and approximation techniques for the optimization tasks, mostly based on machine learning algorithms. For instance, Learning-based MPC addresses the data-driven approximation of possibly different elements of the MPC formulation, such that the overall performance is improved. For these methods, a fundamental categorisation can be made between offline and online paradigms. In offline learning, the model targets the controller design and is trained using synthetic samples, or data obtained from previous simulations [73, 66]. In online learning instead, the model is trained to approximate the system dynamics, and data are collected while the system evolves, hence the model is actively adjusted during the closed-loop operation. Among other methods in this class, we find Gaussian Processes [62, 61, 67] – providing a non-parametric and probabilistic model of the system’s behavior – and Reinforcement Learning [63, 64, 68], particularly useful when the dynamics are complex, unknown, or hard to model accurately using traditional approaches. We refer the reader to [55, 70] for a more comprehensive discussion of the matter.

Here, we limit ourselves to the study of two different approaches. The first one based on a supervised learning MPC, where the control is learned in an off-line phase, over training data generated by sampling optimal trajectories of agents [2, 3, 37]. The second strategy is based on a sequential linearization, where the control is obtained via Riccati-type equations, and re-calibrated dynamically based on a predictive horizon triggered by decay estimate of the agent-system moments [7] in a similar spirit of event-based MPC [40]. Both approaches are based on the realisation of an efficient control for the agent-based dynamics, however the methods are inherently different: the first strategy aims to approximate the optimal control of non-linear dynamics with a bottom-up procedure, while the second strategy determines a minimum intervention to steer non-linear systems towards a desired goal.

The chapter is organized as follows. In Section 2 we introduce the general setting for optimal control of collective dynamics, including first-order optimality conditions and dynamic programming approaches. Section 3 discusses the aforementioned optimal control techniques in the framework of supervised learning, as a method that enables real-time feedback control. Section 4 presents an alternative approach, moment-driven predictive control, which is based on sequential linearization of the dynamics triggered by a macroscopic observable of the particle ensemble. Section 5 concludes with a series of numerical tests illustrating the performance of the different techniques for large-scale particle systems.

2 Optimal control for collective dynamics

Agent-based models are a natural modelling framework to describe behaviour of a group of interacting entities obeying simple rules [69, 27]. In this context, it is of great interest to explore the emergence of self-organizing patterns and collaborative behaviours among agents such as consensus, flocking, mills, etc. Applications include the modelling of language evolution, clustering in opinion dynamics, and collective animal behaviour, among many others. [20, 34, 57, 31, 33].

We consider second-order systems of N interacting agents with state variables described by $s_i = (x_i, v_i) \in \mathbb{R}^d \times \mathbb{R}^d$ for $i = 1 \dots N$, where x_i and v_i represent the position and the velocity of the i -th agent, respectively.

Given an initial configuration of the ensemble, the evolution of the agents is governed by

$$\begin{aligned}\dot{x}_i(t) &= v_i(t), \\ \dot{v}_i(t) &= \frac{1}{N} \sum_{j=1}^N a(\|x_j(t) - x_i(t)\|) (v_j(t) - v_i(t)), \quad i = 1, \dots, N,\end{aligned}\tag{1}$$

where $a \in C^1(\mathbb{R}_+)$ is a non-increasing positive function encoding the interaction kernel. In particular, we focus on kernels of Cucker-Smale type

$$a(r) = \frac{K}{(1+r^2)^\beta}, \quad \beta \geq 0, \quad K > 0.\tag{2}$$

In what follows, for the sake of simplicity, we set $\beta = K = 1$. A remarkable property of the Cucker-Smale model is the emergence of consensus by isotropic averaging, i.e., convergence towards

$$\bar{v} = \frac{1}{N} \sum_{j=1}^N v_j.$$

Consensus convergence depends on the interaction strength, encoded in $a(\cdot)$, and the cohesiveness of the initial configuration [47]. Whenever consensus is not guaranteed to emerge, an external control action can be introduced to enforce convergence towards the desired pattern. To this end, the controlled collective evolution can be modeled as

$$\begin{aligned}\dot{x}_i(t) &= v_i(t), \\ \dot{v}_i(t) &= \frac{1}{N} \sum_{j=1}^N a(\|x_j(t) - x_i(t)\|) (v_j(t) - v_i(t)) + u_i(t),\end{aligned}\tag{3}$$

where each agent is influenced by an ad-hoc control component, with $\mathbf{u}(t) := (u_1, \dots, u_N)^\top$ representing a dynamical external force applied in a centralized manner. This external influence can be tuned by solving an optimal control problem within a set of admissible control signals \mathcal{U} :

$$\mathbf{u}^*(t) = \underset{\mathbf{u}(\cdot) \in \mathcal{U}}{\operatorname{argmin}} \left\{ \mathcal{J}(\mathbf{u}(\cdot)) := \int_0^T \frac{1}{N} \sum_{j=1}^N \left(\|\bar{v}(t) - v_j(t)\|^2 + \gamma \|u_j(t)\|^2 \right) dt \right\},\tag{4}$$

subject to the dynamics (3). In such a way, the control action is designed to penalize both the distance of the agent's velocities from the target \bar{v} and the control energy required to steer the system towards the consensus manifold, with parameter $\gamma > 0$.

Necessary optimality conditions for the optimal control problem (3)-(4) are derived from Pontryagin's Maximum Principle (PMP) [13] leading to a two-point boundary value problem for the state variables s_i , the associated adjoint variables $r_i = (p_i, q_i)$, and the control signals u_i :

$$\begin{cases} \dot{x}_i &= v_i \\ \dot{v}_i &= \frac{1}{N} \sum_{j=1}^N \frac{v_i - v_j}{1 + \|x_i - x_j\|^2} + u_i \\ \dot{p}_i &= -\frac{1}{N} \sum_{j=1}^N \frac{2(x_i - x_j)}{(1 + \|x_j - x_i\|^2)^2} \langle q_j - q_i, v_j - v_i \rangle \\ \dot{q}_i &= -\frac{1}{N} \sum_{j=1}^N \frac{q_j - q_i}{1 + \|x_i - x_j\|^2} - \frac{2}{N} (\bar{v} - v_i) + p_i \end{cases}\tag{5}$$

together with boundary conditions given by $(x_i(0), v_i(0)) = s_i^0$ and $(p_i(T), q_i(T)) = (0, 0)$ for all $i = 1, \dots, N$. The PMP system is closed with the optimality condition

$$\mathbf{u}^*(t) = \underset{u}{\operatorname{argmin}} \left(\sum_{i=1}^N \langle q_i, \dot{v}_i \rangle + \frac{\gamma}{N} \|u_i\|_2^2 \right) = -\frac{N}{2\gamma} \mathbf{q}^\top,\tag{6}$$

where $\mathbf{q} = (q_1, \dots, q_N)^\top$. It is possible to approximate the optimality conditions above by following a reduced gradient approach [54, 13, 12]. Starting with an initial guess for the control signal over the whole horizon, this method iterates forward-backward passes over (5), while updating the control signal $u(\cdot)$ using (6) as a gradient step. Unfortunately, such a method becomes unsuitable for real-time control as the number of agent increases.

2.1 Dynamic programming and the HJB PDE

The problem at hand can be written in a more general form as a finite-horizon optimal control problem for a system of N agents:

$$\min_{\mathbf{u}(\cdot) \in \mathcal{U}} \mathcal{J}(\mathbf{u}(\cdot); t_0, \mathbf{s}) := \int_{t_0}^T \ell(\mathbf{y}(t)) + \frac{\gamma}{N} \|\mathbf{u}(t)\|_2^2 dt, \quad \gamma > 0, \quad (7)$$

subject to nonlinear, control-affine constraint

$$\dot{\mathbf{y}}(t) = f(\mathbf{y}(t)) + g(\mathbf{y}(t))\mathbf{u}(t), \quad \mathbf{y}(t_0) = \mathbf{s}, \quad (8)$$

where the initial condition of the particle ensemble is denoted $\mathbf{s} = (s_1, \dots, s_N)^\top$, with $s_i \in \mathbb{R}^{2d}$, hence the total dimension of the particle system is $n = 2dN$. We define the control variable as $\mathbf{u}(\cdot) \in \mathcal{U} := \{\mathbf{u}(t) : \mathbb{R}_+ \rightarrow \mathbb{R}^m \text{ is measurable}\}$. We further assume the running cost $\ell : \mathbb{R}^n \rightarrow \mathbb{R}$ is continuously differentiable and consider dynamics $f : \mathbb{R}^n \rightarrow \mathbb{R}^n$, $g : \mathbb{R}^n \rightarrow \mathbb{R}^{n \times m}$ in $C^1(\mathbb{R}^n)$.

We solve the optimal control problem (7-8) by means of dynamic programming. For this, we define the value function of the control problem

$$V(t, \mathbf{s}) := \inf_{\mathbf{u}(\cdot) \in \mathcal{U}} \mathcal{J}(\mathbf{u}(\cdot); t, \mathbf{s}), \quad t \in [0, T], \quad (9)$$

which, in the finite-horizon case, satisfies the following Hamilton-Jacobi-Bellman PDE

$$\begin{cases} \partial_t V(t, \mathbf{s}) - \frac{N}{2\gamma} \nabla V(t, \mathbf{s})^\top g(\mathbf{s}) g^\top(\mathbf{s}) \nabla V(t, \mathbf{s}) + \nabla V(t, \mathbf{s})^\top f(\mathbf{s}) + \ell(\mathbf{s}) = 0 \\ V(T, \mathbf{s}) = 0 \end{cases} \quad (10)$$

After solving the HJB PDE above, it is possible to retrieve the optimal control in terms of the gradient of $V(\cdot)$:

$$\mathbf{u}^*(t, \mathbf{s}) = \underset{\mathbf{u} \in \mathbb{R}^m}{\operatorname{argmin}} \left\{ \frac{\gamma}{N} \|\mathbf{u}\|_2^2 + \nabla V(t, \mathbf{s})^\top g(\mathbf{s}) \mathbf{u} \right\} = -\frac{N}{2\gamma} g^\top(\mathbf{s}) \nabla V(t, \mathbf{s}), \quad (11)$$

In this way, the control design is in feedback form $\mathbf{u}^* = \mathbf{u}^*(t, \mathbf{s}(t))$, associating an optimal action to every state. However, equation (10) is a fully nonlinear, first-order PDE lacking a generally applicable explicit solution. Moreover, the HJB equation is cast over the state space of the system dynamics, which can potentially be of arbitrarily high dimensions – especially in the context of multi-agent systems, in which the dimensionality scales with both the number N of agents and the dimension d of the underlying state space. Following previously introduced notation, the ensemble state \mathbf{s} encompasses $2dN$ entries. Bellman himself coined the term *curse of dimensionality* to describe the challenges associated to the computational complexity of solving dynamic programming equations, which becomes particularly evident in large-scale interacting particle systems. In this context, we will discuss computational approaches to circumvent the solution of high-dimensional HJB equations.

2.2 The link between PMP and HJB

In this section we investigate the connection between Pontryagin Maximum Principle and Dynamic Programming for optimal control design. The approaches are inherently different, as PMP yields open-loop controls satisfying a necessary first order optimality system, whilst solutions of the HJB equation are associated with feedback laws that meet both necessary and sufficient optimality conditions. The finite-horizon optimal control problem (7-8) is associated with Hamiltonian

$$H(t, \mathbf{s}, \mathbf{u}, \mathbf{r}) = \left(f(\mathbf{s}(t)) + g(\mathbf{s}(t))\mathbf{u}(t) \right)^\top \mathbf{r} + \ell(\mathbf{s}(t)) + \frac{\gamma}{N} \|\mathbf{u}(t)\|_2^2, \quad (12)$$

which is defined as a function of ensemble state \mathbf{s} , control \mathbf{u} , and adjoint variable $\mathbf{r} := (\mathbf{p}, \mathbf{q})$, appearing in this formulation as a time-dependent Lagrange multiplier.

Pontryagin's principle states requirements that must hold along any optimal trajectory $(\mathbf{s}^*, \mathbf{u}^*, \mathbf{r}^*)$, formulated as the following two-point boundary value problem (TPBVP)

$$\begin{cases} \dot{\mathbf{s}}^*(t) &= \partial_{\mathbf{r}} H(t, \mathbf{s}^*, \mathbf{u}^*, \mathbf{r}^*) \\ \dot{\mathbf{r}}^*(t) &= -\partial_{\mathbf{s}} H(t, \mathbf{s}^*, \mathbf{u}^*, \mathbf{r}^*) \\ \mathbf{s}^*(0) &= \mathbf{s}_0, \quad \mathbf{r}^*(T) = 0, \end{cases} \quad (13)$$

and closed with the first order optimality condition for the optimal control:

$$\mathbf{u}^*(t) = \partial_{\mathbf{u}} H(t, \mathbf{s}^*, \mathbf{u}^*, \mathbf{r}^*) = \frac{N}{2\gamma} g^\top(\mathbf{s}^*(t)) \mathbf{r}^*(t). \quad (14)$$

Note that this procedure only provides necessary conditions for optimality, meaning that PMP solutions identify stationary points of $\partial_{\mathbf{u}} H$, with only some of them being global minimizers. Triples $(\mathbf{s}^*, \mathbf{u}^*, \mathbf{r}^*)$ solving (13-14) are called *extremal trajectories*, and are computed from a fixed initial configuration \mathbf{s}_0 , hence they are not in feedback form.

The connection between Pontryagin's and Bellman's principles in finite horizon settings has been investigated since the early works of analysis in optimal control [74]. Under suitable assumptions on the regularity of the HJB solution (here $V \in C^1$), it can be shown that the forward-backward dynamics derived in PMP serve as characteristic curves for the HJB equation [81, 76]. Consequently, the value function associated with the optimal control problem can be determined at a specific state-space point \mathbf{s} by solving the TPBVP (13) from the initial condition \mathbf{s}_0 and integrating along the resulting optimal trajectory, its gradient being the adjoint variable [16, 29, 15]:

$$V(t, \mathbf{s}_0) = \int_{t_0}^T \ell(\mathbf{s}^*) + \frac{\gamma}{N} \|\mathbf{u}^*(t)\|_2^2 dt, \quad \nabla V(t, \mathbf{s}_0) = \mathbf{r}^*(t). \quad (15)$$

A typical objective in MPC is asymptotic stabilization, which is expressed as an *infinite* horizon optimal control problem, to which the previous interpretation does not readily extend as the final condition for the adjoint variable is pathologically set at infinity. Several methods have been proposed in the literature to let $T \rightarrow \infty$ within PMP [23]; in this present work, we consider a finite horizon T *long enough* [11] for the system to reach consensus. In particular, we rely on long-horizon open-loop solves departing from the current system configuration \mathbf{s} , and retrieve a control action of feedback nature by associating the first time instance of the control signal to the state \mathbf{s} [?]. As investigated in [65], this receding horizon strategy can be used as a relaxation of the Dynamic Programming approach.

2.3 State Dependent Riccati Equation

An alternative approach for solving the infinite horizon optimal control problem is to approximate the solution of the associated dynamic programming HJB equation. We consider a quadratic cost

$$\min_{\mathbf{u}(\cdot) \in \mathcal{U}} \mathcal{J}(\mathbf{u}(\cdot), \mathbf{y}) := \int_0^\infty \mathbf{s}^\top(t) Q \mathbf{s}(t) + \mathbf{u}^\top(t) R \mathbf{u}(t) dt, \quad (16)$$

subject to control-affine dynamical constraints (8). The matrix $Q \in \mathbb{R}^{n \times n}$ and $R \in \mathbb{R}^{m \times m}$ are assumed to be symmetric, such that $Q \succeq 0$, $R > 0$. We further assume $f(0) = 0$, $g(0) = 0$. Accordingly, the optimal value function

$$V(\mathbf{s}) := \inf_{\mathbf{u}(\cdot) \in \mathcal{U}} \mathcal{J}(\mathbf{u}(\cdot), \mathbf{s}) \quad (17)$$

satisfies the following Hamilton-Jacobi-Bellman equation

$$\nabla V(\mathbf{s})^\top f(\mathbf{s}) - \frac{1}{4} \nabla V(\mathbf{s})^\top g(\mathbf{s}) R^{-1} g(\mathbf{s})^\top \nabla V(\mathbf{s}) + \mathbf{s}^\top Q \mathbf{s} = 0 \quad (18)$$

with optimal feedback control

$$\mathbf{u}(\mathbf{s}) = -\frac{1}{2}R^{-1}g(\mathbf{s})^\top \nabla V(\mathbf{s}). \quad (19)$$

To circumvent directly solving the HJB PDE (18) for V , we resort to the State Dependent Riccati Equation (SDRE) approach, providing suboptimal feedback laws that ensure local stability. The SDRE method can be applied for system dynamics represented in semi-linear form

$$\dot{\mathbf{s}} = A(\mathbf{s})\mathbf{s} + B(\mathbf{s})\mathbf{u}(t), \quad (20)$$

provided that the pair $(A(\mathbf{s}), B(\mathbf{s}))$ is stabilizable for all $\mathbf{s} \in \mathbb{R}^n$ [10]. The SDRE approach is based on the idea that the value function (17) is non-negative by construction, and with no loss of generality it can be represented as a quadratic form $V(\mathbf{s}) = \mathbf{s}^\top \Pi(\mathbf{s})\mathbf{s}$, with $\Pi(\cdot) \in \mathbb{R}^{n \times n}$ a symmetric matrix-valued function. By approximating $\nabla V(\mathbf{s}) = 2\Pi(\mathbf{s})\mathbf{s}$ and inserting it into the HJB equation (18), we obtain the State-dependent Riccati Equation

$$A^\top(\mathbf{s})\Pi(\mathbf{s}) + \Pi(\mathbf{s})A(\mathbf{s}) - \Pi(\mathbf{s})B(\mathbf{s})R^{-1}B^\top(\mathbf{s})\Pi(\mathbf{s}) + Q = 0 \quad (21)$$

to be solved for $\Pi(\mathbf{s})$. The resulting feedback law then reads

$$\mathbf{u}(\mathbf{s}) = -R^{-1}B^\top(\mathbf{s})\Pi(\mathbf{s})\mathbf{s}. \quad (22)$$

The SDRE feedback law is suboptimal compared to the solution of the HJB equation (18), as the semi-linearization $f(\mathbf{s}) = A(\mathbf{s})\mathbf{s}$ is not unique. More substantially, equation (21) holds for the approximation of $\nabla V(\mathbf{s}) \approx 2\Pi(\mathbf{s})\mathbf{s}$, whereas a chain rule calculation shows

$$[\nabla V(\mathbf{s})]_k = 2\Pi(\mathbf{s})\mathbf{s} + \sum_{i,j} s_i s_j \partial_{s_k} \Pi_{i,j}(\mathbf{s}). \quad (23)$$

These two aspects are in no way independent, as one could optimize the choice of $A(\cdot)$ in such a way that minimizes the misfit between the SDRE and the HJB feedback laws [58, 36].

2.3.1 Frozen Riccati Approach

The state dependency of the operator $\Pi(\mathbf{s})$ in (21) suggests that the computational complexity associated with the SDRE solution is indeed similar to the original HJB (18). We follow a similar approach as in [14], realizing the feedback design in a model predictive control fashion: given the current configuration \mathbf{s} of the system, we freeze the operator $\Pi(\mathbf{s}) \equiv \Pi \in \mathbb{R}^{n \times n}$, meaning that (21) reduces to its algebraic form, where all the state dependencies are neglected by accordingly evaluating all the operators at \mathbf{s}

$$\Pi = Q + A^\top \Pi A - A^\top \Pi B (R + B^\top \Pi B)^{-1} B^\top \Pi A. \quad (24)$$

The system is then evolved for a short time, after which the current state \mathbf{s} is updated. This procedure requires subsequently solving the linear quadratic problem associated with the frozen system, which is addressed via the linear quadratic regulator routine.

2.3.2 Semilinearization of the Cucker-Smale consensus problem

The semi-linear formulation of the dynamics of interest is derived for the ensemble configuration \mathbf{s} , where a two-dimensional agent's state is denoted as $(x, v) = (x^1, x^2, v^1, v^2)$:

$$\mathbf{s} := \left(x_1^1, x_1^2, \dots, x_N^1, x_N^2, v_1^1, v_1^2, \dots, v_N^1, v_N^2 \right)^\top, \quad (25)$$

and it holds as in (20) for operators: $B = (\mathbb{O}_{2n}, \mathbb{I}_{2n})^\top$,

$$A(\mathbf{s}) = \begin{bmatrix} \mathbb{O}_{2n} & \mathbb{I}_{2n} \\ \mathbb{O}_{2n} & \tilde{A}(\mathbf{s}) \end{bmatrix} \quad \tilde{A}_{i,j}(\mathbf{s}) = \begin{cases} a(\|x_j - x_i\|) & \text{if } i \text{ odd, } j = i + 1 \\ a(\|x_j - x_i\|) & \text{if } i \text{ even, } j = i - 1 \\ -a(\|x_j - x_i\|) & \text{if } i = j \\ 0 & \text{otherwise} \end{cases} \quad (26)$$

where $\mathbb{O}_{2n}, \mathbb{I}_{2n}$ indicate the zero and the identity matrices in $\mathbb{R}^{2n \times 2n}$ respectively, $n = dN$, and a Cucker-Smale type kernel defined in (2). Furthermore, aiming at writing the consensus cost functional as in (16), we notice that

$$\sum_{i=1}^N \|v_i - \bar{v}\|^2 = \|\mathbf{v} - C\mathbf{v}\|^2 \quad (27)$$

for $\mathbf{v} = (v_1, \dots, v_N)^\top$ and a matrix $C \in \mathbb{R}^{n \times n}$ full of zeros, except for the $N \times N$ diagonal blocks, which are valued $N^{-1} \cdot \mathbb{1}_N$, for $\mathbb{1}_N$ denoting a matrix in $\mathbb{R}^{N \times N}$ full of ones. It follows that

$$\|\mathbf{v} - C\mathbf{v}\|^2 = \mathbf{v}^\top \left(\mathbb{I}_n + C^\top C - 2C \right) \mathbf{v}. \quad (28)$$

Thus, we can write the cost (4) in the form (16) w.r.t. linear operators

$$Q = \mathbb{I}_n + C^\top C - 2C, \quad R = \frac{\gamma}{N} \cdot \mathbb{I}_n. \quad (29)$$

3 Supervised learning MPC approach

When working with high-dimensional problems, both of the PMP and SDRE approaches for control synthesis may still require considerable CPU times to be implemented in the receding horizon framework. To alleviate this issue, we rely on data-driven supervised learning methods to provide an offline approximation of the feedback law, enabling real-time control.

In the context of regression analysis, our primary goal is to approximate the control action by instructing the model through dataset training, effectively establishing a mapping from system configurations to the target variable of interest, which is either the value function or the feedback control.

Our discussion will proceed as follows: we will start by addressing the generation of synthetic data and the selection of the target for approximation, then introduce the neural network architecture and training, to conclude by exploring its real-time application in a receding horizon fashion.

3.1 Gradient-augmented regression and data generation

We aim at providing a model $\tilde{\mathbf{u}} \approx \mathbf{u}$ acting as a surrogate of the feedback law to accelerate the receding horizon control of the system at hand. Being the synthesis of the control action the objective of the learning operation, the first candidate for approximation is the state-to-control map $\mathbf{s} \mapsto \mathbf{u}(\mathbf{s})$.

As an alternative, another quantity of interest is the value function V , from where a control can be derived from $\mathbf{u} \approx \nabla V$, according to the optimality conditions in equation (19) and (14). Besides its theoretical significance, a key advantage of selecting V as a learning objective is its property of being a scalar function, hence relatively easy to approximate. Note that information about ∇V is generated for free as a byproduct of both the SDRE and PMP routines. In the SDRE case, this resides in the ansatz $\nabla V(\mathbf{s}) \approx 2\Pi(\mathbf{s})\mathbf{s}$, expressed in terms of the solution operator $\Pi(\cdot)$; in PMP instead, the gradient of the value function coincides with the adjoint variable \mathbf{r} . Both the learned (and V -learned) control designs will be compared learning objectives, depending on the sampling of a suitable training dataset.

We sample state configurations $\{\mathbf{s}^{(i)}\}_{i=1}^{N_s}$ and couple them with the associated labels $\mathbf{u}^{(i)} := \mathbf{u}(\mathbf{s}^{(i)})$, $V^{(i)} := V(\mathbf{s}^{(i)})$, $\nabla V^{(i)} := \nabla V(\mathbf{s}^{(i)})$:

- In the PMP framework, we solve the optimality system (5-6) fixing each sample as initial configuration $\mathbf{y} = \mathbf{s}^{(i)}$. As done in [12], once the extremal trajectory $(\mathbf{s}^*, \mathbf{u}^*, \mathbf{r}^*)$ is computed for time $t \in [0, T]$, the variables of interest can be obtained as follows: the feedback control associated with the initial condition $\mathbf{s}^{(i)}$ is $\mathbf{u}^{(i)} = \mathbf{u}^*(t=0)$, the optimal cost-to-go from $\mathbf{s}^{(i)}$ can be retrieved as the cost integrated along the extremal trajectory, and coincides with the value function $V^{(i)} = V(\mathbf{s}^{(i)}, t=0)$, its gradient being $\nabla V^{(i)} = \mathbf{r}^*(t=0)$.
- For the SDRE approach, we solve the Algebraic Riccati Equation (24) associated with freezing (21) at each current state $\mathbf{s}^{(i)}$. The target variables can then be retrieved by using the quadratic ansatz for $V^{(i)} = \mathbf{s}^{(i)\top} \Pi(\mathbf{s}^{(i)}) \mathbf{s}^{(i)}$, $\nabla V^{(i)} = 2\mathbf{s}^{(i)\top} \Pi(\mathbf{s}^{(i)})$ and the first order optimality condition for \mathbf{u} in (22) [2, 3].

3.2 Feedforward Neural Networks

We limit our the discussion to models belongings to the class of fully connected Feedforward Neural Networks. These models approximate generic functions ϕ by chains of composition of layer maps l_1, \dots, l_M , i.e., $\tilde{\phi} = \phi_\theta \approx \phi$ with

$$\phi_\theta(z) = l_M \circ \dots \circ l_2 \circ l_1(z), \quad z \in \mathbb{R}^n,$$

during which the information flows from the input nodes to the output ones in a unidirectional path, avoiding any cycles or loops. For $m = 1, \dots, M$, the layer l_m is defined as $l_m(z) = \sigma_m(A_m z + b_m)$, where the nonlinear activation function $\sigma_m : \mathbb{R}^n \rightarrow \mathbb{R}$ is applied component-wise to a linear combination of the layer input variable, with $A_m \in \mathbb{R}^{n \times n}$ and $b_m \in \mathbb{R}^n$ being weight matrix and bias vector for the m -th layer respectively.

Considering a data set $\mathcal{T} = \{z^{(i)}, \phi^{(i)} := \phi(z^{(i)})\}_{i=1}^{N_s}$, the $\theta = \{A_m, b_m\}_{m=1}^M$ are trainable parameters to be optimized according to a loss function \mathcal{L} in a supervised learning fashion

$$\theta = \arg \min_{\theta} \sum_{z \in \mathcal{T}} \mathcal{L}(\phi(z), \phi_\theta(z)).$$

In our setting, we rely on the mean squared error (MSE) as measure of the approximation error \mathcal{L}_0 . In the gradient-augmented regression for V , we penalize the discrepancy with respect to the derivative information as well:

$$\begin{aligned} \mathcal{L}_0(\phi, \phi_\theta) &= \sum_{i=1}^{N_s} \frac{\|\phi^{(i)} - \phi_\theta(z^{(i)})\|^2}{N_s}, \\ \mathcal{L}_1(\phi, \phi_\theta) &= \mathcal{L}_0(\phi, \phi_\theta) + \mu \mathcal{L}_0(\nabla \phi, \nabla \phi_\theta). \end{aligned} \quad (30)$$

The number of layers M , the number of neurons per layer (width of layer), the activation functions $\sigma_m(\cdot)$ in the hidden layers and the loss weight μ are hyper-parameters which need to be optimally tuned according to the model's goodness of fit, so that the trained model adapt properly to new, previously unseen data.

3.3 MPC with the learned feedback control

Once the models $\tilde{\mathbf{u}}$ are trained over the synthetically generated data, they can be used as numerical representations of the optimal feedback control law. Defining an uniformly spaced time-discretization with a step size δ on the time interval $[0, T]$ by $t_h = h\delta$, $h = 1, \dots, T/\delta$, we denote $\mathbf{s}^h := \mathbf{s}(t_h)$. Departing from the initial configuration of the system $\mathbf{s}_0 = \mathbf{y}$, we follow a receding horizon strategy for the controlled evolution

$$\mathbf{s}^{h+1} = \mathbf{s}^h + \delta \left(f(\mathbf{s}^h) + g(\mathbf{s}^h) \tilde{\mathbf{u}}(\mathbf{s}^h) \right). \quad (31)$$

This allows to replace the subsequent calls to optimal control solvers by mere model evaluations, leading to a considerable complexity reduction, as shown in terms of CPU speed-up in the numerical test section.

4 Moment-driven predictive control

We propose an additional approach to avoid the limitations associated with the synthesis of optimal feedback laws for high-dimensional non-linear dynamics through conventional approaches, like the computationally expensive solution of the Hamilton-Jacobi-Bellman PDE. To his end, we present a sub-optimal feedback-type control through the linearization of the interaction kernel, and solve the resulting linear-quadratic optimal control problem through a Riccati equation. The proposed methodology yields a control law for the linear model, which is later embedded into the non-linear dynamics. The proposed design only requires recurrent measurements of the nonlinear state. No continuous estimation of the nonlinear state or the synthesis of a nonlinear feedback is necessary. The approach relies on the fact, that the linearized system could be controlled efficiently using a Riccati formulation.

However, using the linear optimal control within the nonlinear model does not necessarily yield a stabilizing control law, since over time the nonlinear dynamics may be far from the linearization point. Because of the latter, we aim to quantify the impact of this control. This will determine the number of linearization updates needed to

stabilize the nonlinear system. The performance is quantified by estimating the decay of macroscopic quantities such as the second moment of the particle ensemble.

This framework, called Moment-driven Predictive Control (MdPC) is based on the work [7]. Using dynamic estimates of the moments decay, a forward error analysis is performed to estimate the next linearization point.

Moreover, the proposed control strategy is capable of treating efficiently high-dimensional non-linear control problems due to the Riccati approach employed for the linearized system.

4.1 Riccati-based open-loop control

We consider a linearization-based approach for the finite horizon minimization problem introduced in Section 2. In this new approach, the non-linear dynamics (3) is linearized for every agent around an equilibrium (\tilde{x}, \tilde{v}) . We assume that the communication function a evaluated at the equilibrium is such that $a(0) \equiv \bar{p}$, for some $\bar{p} > 0$. Introducing the shift $z_i = x_i - \tilde{v}t$, $w_i = v_i - \tilde{v}$, we obtain the linearized system

$$\begin{aligned} \dot{z}_i(t) &= w_i(t), & z_i(0) &= x_i(0), \\ \dot{w}_i(t) &= \frac{1}{N} \sum_{j=1}^N \bar{p} (w_j(t) - w_i(t)) + u_i(t), & w_i(0) &= v_i(0) - \tilde{v}, \end{aligned}$$

For the sake of compactness, and differently from the previous section, here we consider the full states of the interacting agent system as $z(t), w(t), u(t) \in \mathbb{R}^{N \times d}$, i.e. the position and velocity of each i -agent are stored by row. Hence, we can write in matrix-vector notation

$$\begin{bmatrix} \dot{z}(t) \\ \dot{w}(t) \end{bmatrix} = \begin{bmatrix} \mathbb{O}_N & \mathbb{I}_N \\ \mathbb{O}_N & P \end{bmatrix} \begin{bmatrix} z \\ w \end{bmatrix} + \begin{bmatrix} \mathbb{O}_N \\ \mathbb{I}_N \end{bmatrix} u,$$

where the matrix $P \in \mathbb{R}^{N \times N}$ is defined as

$$(P)_{ij} = \begin{cases} \frac{\bar{p}(1-N)}{N}, & i = j, \\ \frac{\bar{p}}{N}, & i \neq j, \end{cases} \quad i, j = 1 \dots, N. \quad (32)$$

This second-order system is controllable [50] and since it is linear, the optimal control problem is solved using the Riccati equation. We focus on the case where the average velocity in the cost (4) is a fix target, i.e. $\bar{w} = 0$. The exact solution is given as state feedback by

$$u(t) = -\frac{N}{\gamma} K_{22}(t) w(t), \quad (33)$$

where $K_{22} \in \mathbb{R}^{N \times N}$ is associated to the solution of the following differential Riccati matrix-equation

$$\begin{aligned} - \begin{bmatrix} \dot{K}_{11} & \dot{K}_{12} \\ \dot{K}_{21} & \dot{K}_{22} \end{bmatrix} &= \begin{bmatrix} \mathbb{O}_N & \mathbb{O}_N \\ \mathbb{O}_N & K_{21} + K_{22}P \end{bmatrix} + \begin{bmatrix} \mathbb{O}_N & \mathbb{O}_N \\ K_{11} + PK_{21} & K_{12} + PK_{22} \end{bmatrix} \\ &\quad - \frac{N}{\gamma} \begin{bmatrix} K_{12}K_{21} & K_{12}K_{22} \\ K_{22}K_{21} & K_{22}K_{22} \end{bmatrix} + \begin{bmatrix} \mathbb{O}_N & \mathbb{O}_N \\ \mathbb{O}_N & \mathbb{I}_N \end{bmatrix}, \end{aligned}$$

with terminal conditions $K_{ij}(T) = \mathbb{O}_N$, for $i, j = 1, 2$. This system is easily solved with $K_{11} = K_{12} = K_{21} = \mathbb{O}_N$ and K_{22} fulfilling

$$-\dot{K}_{22} = K_{22}P + PK_{22} - \frac{N}{\gamma} K_{22}K_{22} + \mathbb{I}_N, \quad K_{22}(T) = \mathbb{O}_N. \quad (34)$$

For a general linear system, we need to solve the $N \times N$ differential system (34), which can be costly for large-scale agent-based dynamics. However, we exploit the symmetric structure of the matrix P to reduce the dimension of the Riccati equation considering K_{22} parametrized with a diagonal element $k_d(t)$ and an off-diagonal element $k_o(t)$, according to the approach in [7, 52], as follows

$$(K_{22})_{ij} = \delta_{ij} N k_d(t) + (1 - \delta_{ij}) N^2 k_o(t), \quad i, j = 1, \dots, N,$$

with δ_{ij} indicating the Kronecker delta. Hence, we have the following

Proposition 1 For the linearized dynamics, the solution of the Riccati equation (34) reduces to the solution of

$$-\dot{k}_d = -2\bar{p}\alpha(N) \left(k_d - \frac{k_o}{N} \right) - \frac{1}{\nu} \left(k_d^2 + \frac{\alpha(N)}{N} k_o^2 \right) + 1, \quad k_d(T) = 0, \quad (35a)$$

$$-\dot{k}_o = 2\bar{p} \left(k_d - \frac{k_o}{N} \right) - \frac{1}{\nu} \left(2k_d k_o + \alpha(N) k_o^2 - \frac{1}{N} k_o^2 \right), \quad k_o(T) = 0, \quad (35b)$$

with terminal conditions $k_d(T) = k_o(T) = 0$, and where $\alpha(N) = \frac{N-1}{N}$.

The state feedback (33) is given by

$$u_i(t) = -\frac{1}{\gamma} \left(\left(k_d(t) - \frac{k_o(t)}{N} \right) w_i(t) + \frac{k_o(t)}{N} \sum_{j=1}^N w_j(t) \right). \quad (36)$$

We refer to [7] for the proof of Proposition 1 and further details regarding this approach.

In order to approximate the synthesis of feedback laws for the original non-linear optimal control problem, we study sub-optimal stabilizing strategies induced by the feedback (36). In a feed forward approach we apply (36) directly in the nonlinear dynamics. This is an open-loop type of control, since all the information on the state of the non-linear system reduces to the initial state of the linearized system, assuming $w_i(0) = v_i(0)$. While it is clearly outperformed by an optimal feedback law in terms of robustness, it has the advantage that it can be implemented without requiring a continuous measurement of the full nonlinear state $v(t)$, making it appealing for systems where recovering the true state of the dynamics can be expensive or time-consuming. This stabilization strategy is clearly suboptimal with respect to the original optimal control problem, and in general will not guarantee the stabilization of the non-linear dynamics (3). In order to estimate these performances in the case where a large number of agents is present, i.e. $N \gg 1$, we conduct the error analysis from a *mean-field* perspective.

4.2 Moments estimates for error analysis

We consider the probability density distribution of agents to describe the collective behavior of a large ensemble of agents, and retrieve upper and lower bounds for the decay of the mean-field density towards the desired configuration. For further details on mean-field derivation of particle systems we refer to [7, 26, 25, 22] as well as to [43, 42] for rigorous results on the convergence. We denote by $f(t, z, w)$ and $g(t, x, v)$ the mean-field probability densities corresponding to the linear and non-linear dynamics, respectively. The detailed equations are stated in [7]. The performance of the MdPC approach relies on estimates of the variance of g . For given initial data $g^0 := g(0, x, v)$, we have the following result

Proposition 2 Assume the kernel $a(\cdot)$ to be a bounded function, namely

$$a(r) \in [-\alpha, \beta], \quad \alpha, \beta \geq 0.$$

We have the following lower and upper bounds for the evolution of the variance $\sigma^2[g]$:

$$\begin{aligned} \sigma^2[g^0] e^{-2\beta t} \left(1 - B_\beta^+(0, t) \right)^2 &\leq \sigma^2[g](t) \leq \sigma^2[g^0] e^{2\alpha t} \left(1 + B_\alpha^-(0, t) \right)^2, \quad \text{where} \\ B_c^\pm(t_0, t) &= \frac{1}{\nu} \int_{t_0}^{t-t_0} \eta(s-t_0) k_d(s) e^{\pm c(s-t_0)} ds, \\ \eta(t-t_0) &= \exp \left\{ -2\bar{p}(t-t_0) - \frac{1}{\nu} \int_{t_0}^{t-t_0} k_d(r) dr \right\}. \end{aligned}$$

4.3 MdPC approach

Relevant issues in the MPC literature are the selection of suitable intermediate time horizons that can ensure asymptotic stability, as well as the design of effective optimization methods, such that the implementation is suitable for real-time control. We propose a MPC-type algorithm where instead of fixing a prediction horizon, the

re-calibration of the control law introduced in Section 4.1 is triggered adaptively in time. This is based on a direct estimate of the decay of the variance estimated above.

Starting by the control (36) we consider densities at initial time given by $g(0, x, v) = g^0(x, v)$, $f^0(x, v) \equiv g^0(x, v)$. Prediction of the error in the variance decay $\sigma^2[g](t)$ is given by Proposition 2 that yields

$$\Delta_\sigma(t_0, t) = \sigma^2[g(t_0, x, v)] \left(e^{2\alpha(t-t_0)} (1 + B_\alpha^-(t_0, t))^2 - e^{-2\beta(t-t_0)} (1 - B_\beta^+(t_0, t))^2 \right).$$

Then, $\Delta_\sigma(t_0, t)$ is used to guarantee the variance of g is below a fixed threshold $\delta_{tol} > 0$. This defines a time $t_1 > t_0$ such that $\Delta_\sigma(t_0, t_1) > \delta_{tol}$. Once we reach the threshold, we reinitialize by updating the state of the linearized dynamics at time t_1 by setting $f(t_1, x, v) \equiv g(t_1, x, v)$ and repeat the procedure, see Algorithm 1.

Algorithm 1 [MdPC]

0. Set $k \leftarrow 0$, $t_k = 0$, $g^k(x, v) = g(0, x, v)$, $f^k(x, v) = g(0, x, v)$ and tolerance δ_{tol}
1. Solve the Riccati equation to obtain k_d , k_o on the time interval $[0, T]$
2. Find the time t_{k+1} such that $t_{k+1} := \min\{t | t_k < t \leq T, \Delta_\sigma(t_k, t) > \delta_{tol}\}$
- while** $t_{k+1} \leq T$ **do**

 - i. Evolve the linear and non-linear dynamics up to t_{k+1}
 - ii. Set $g_{k+1}(x, v) = g(t_{k+1}, x, v)$, $f_{k+1}(x, v) = g(t_{k+1}, x, v)$
 - iii. $k \leftarrow k + 1$
 - iv. Compute t_{k+1} from step 2

- end while**

5 Numerical Tests

We apply the proposed methodologies to the high-dimensional second-order consensus problem (4) for a system of $N = 50$ agents in \mathbb{R}^2 , following dynamics of Cucker-Smale type (3) and a control penalization parameter $\gamma = 0.1$. We consider the integration of the system in a time-frame $t \in [0, T]$ with $T = 10$ and time-step $\delta = 0.01$. The solution of this optimal control problem is associated with an HJB equation cast in a $2dN = 200$ dimensional space, hence the need to rely on numerical representations for the optimal feedback design.

5.1 Test 1: Supervised Learning MPC

In this first numerical example, we test the neural network approximation presented in Section 3. Once the training data are collected, we train models for both the control designs and target variables, denoted as:

- \mathbf{u}_θ^{SDRE} , \mathbf{u}_θ^{PMP} – for the direct approximation of the mapping $x \mapsto u(x)$;
- \mathbf{u}_V^{SDRE} , \mathbf{u}_V^{PMP} – for the approximation of the feedback map through a model for the value function V . In this case, a deterministic layer is stacked on top of the FNN, encoding (14,19).

We prescribe the initial condition for the ensemble state $\mathbf{s} \in [0, 1]^{2dN}$, and a grid search in the parametric space is performed, to select an appropriate model architecture. In Table 1, we compare the architectures of the different models, characterized by the number M of layers, the width of each one of them, the activation functions σ on the hidden layers and the gradient augmentation parameter μ . All models have been trained with the Adam solver [60] over batches of 200 samples. In the table, we also display the Coefficient of Variation or Percent Root Mean Squared Error (PRMSE) for the different models when applied to a testing dataset of 10^6 unseen sample initial conditions in $[0, 1]^{2dN}$.

In Figure 1 a plot of the distance from the target configuration is displayed for the different models, and compared with the one resulting from both the PMP approach and the frozen SDRE, in a simulation in times $t \in [0, 10]$, with $\delta = 0.01$ seconds.

Another interesting comparison is the one in terms of the required CPU time for integrating the system trajectories while controlling them via the different methods. This is presented in Table 2, versus the CPU time used by the forward simulation with the original solvers.

	M	layers width	σ	μ	PRMSE
\mathbf{u}_θ^{SDRE}	1	1000	tanh	—	0.7921%
\mathbf{u}_θ^{PMP}	3	400	sigmoid	—	1.1477%
\mathbf{u}_V^{SDRE}	2	200, 100	sigmoid	0.07	4.1843%
\mathbf{u}_V^{PMP}	2	800	sigmoid	0.1	4.8775%

Table 1: **Test 1:** Different model specifics, including architectural details and Percent RMSE in a test-set.

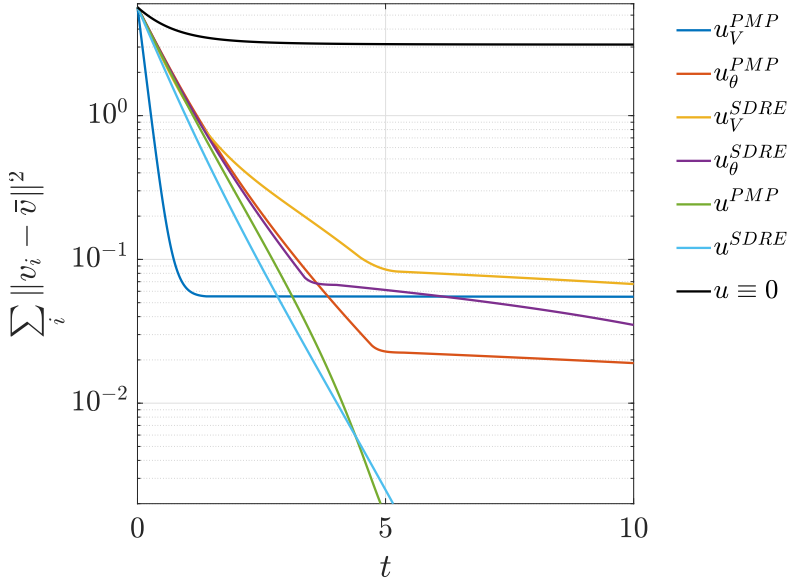


Figure 1: **Test 1:** Comparison of learned and target trajectories for a random initial condition in $[0, 1]^{2dN}$. All the models improve consensus with respect to the uncontrolled dynamics. In terms of learned models, the \mathbf{u}_V^{PMP} model can be considered the optimal one, with an overall cost (at final time horizon T) $\mathcal{J} \approx 1.44$.

5.2 Test 2: MdPC for the Cucker-Smale model

For the second experiment, we employ the MdPC method outlined in Section 4 to address the high-dimensional control problem given by (4) along with the constraint (3). Using the Cucker-Smale interaction kernel and maintaining the parameters from Test 1, we modify the initial velocities while keeping the positions initialized as before, i.e., $v_i(t)$ uniformly distributed in the interval $[-1, 1]$ and $x_i(t)$ in $[0, 1]$. The control is determined through the MdPC algorithm 1, and we use Proposition 1 to derive the corresponding Riccati equations. We conduct a numerical investigation about the decay of the variance σ^2 with varying tolerances δ_{tol} .

In the left panel of Figure 3, various control actions are compared based on target distance, as in Figure 1 from Test 1. Notably, the decay is more pronounced in the presence of control and with a smaller tolerance δ_{tol} . This is due to the fact that we have more information about the non-linear dynamics as the tolerance decreases.

\mathbf{u}_θ^{SDRE}	\mathbf{u}_θ^{PMP}	\mathbf{u}_V^{SDRE}	\mathbf{u}_V^{PMP}	SDRE	PMP
13.9152	9.2503	11.8068	4.0699	1821.21	425.1578

Table 2: **Test 1:** CPU time (in seconds) required for the system integration along time $t \in [0, 10]$ under the different alternative feedback designs.

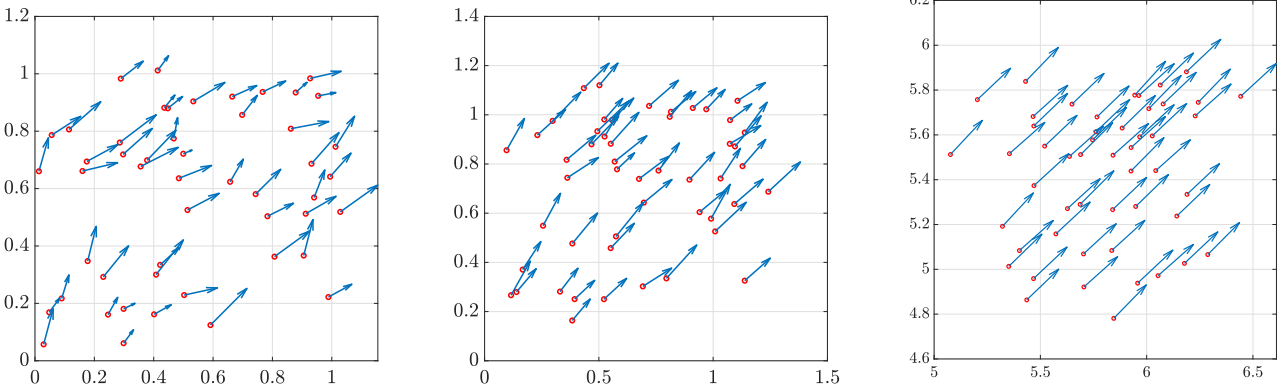


Figure 2: **Test 1:** System configuration at time $t = 0, 1, 10$ seconds respectively, under the control action provided by the feedback map \mathbf{u}_V^{PMP} .

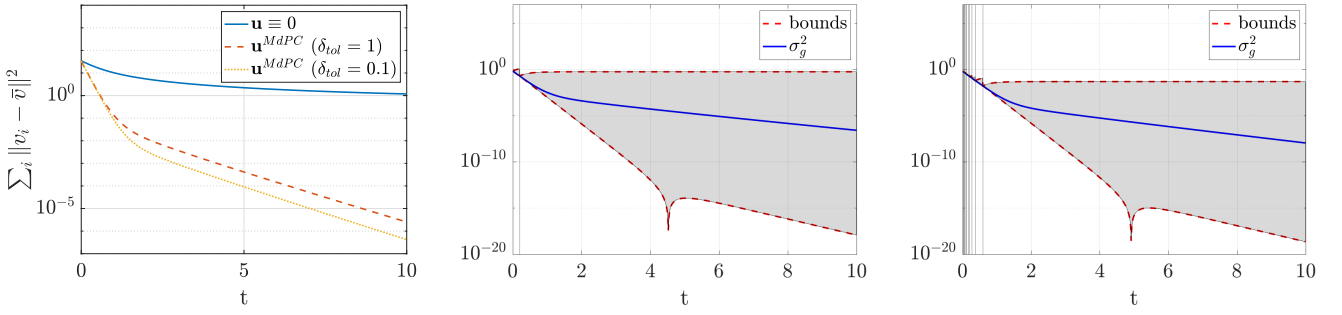


Figure 3: **Test 2:** On the left, comparison of MdPC-controlled and uncontrolled trajectories in terms of particles' target distance. Variance decay together with updates and variance bounds in the middle ($\delta_{tol} = 1$) and on the right ($\delta_{tol} = 0.1$).

The center and right panels of Figure 3 depict the variance decay for $\delta_{tol} = 1$ and $\delta_{tol} = 0.1$ respectively. Black vertical lines represent updates, while dashed red lines illustrate the evolution of the variance bounds. The decay is stronger, and the bounds are stricter with a smaller δ_{tol} . For $\delta_{tol} = 1$, only one update is required, corresponding to a single-step observation of the non-linear dynamics (refer to Algorithm 1). While with $\delta_{tol} = 0.1$, there are 10 updates over a total of 1000 time-steps.

In Figure 4, the evolution of positions and velocities is illustrated through three snapshots: the initial data at $t = t_0 = 0$ on the left, an intermediate time-step at $t = 1$ in the center, and the final configuration at $t = T = 10$ on the right. The initial mean velocity is zero and the objective is to achieve consensus, hence all final velocities are uniformly zero as expected.

We conclude the analysis by presenting the computational times in Table 3.

Using the Riccati equation for control synthesis yields an optimal control for cost functionals associated with linear dynamics only. However, in the more general non-linear case, such control becomes sub-optimal, as evidenced in previous works such as [6, 53]. We emphasize that the MdPC approach offers an adaptive synthesis of sub-optimal feedback controls specifically designed for non-linear dynamics.

Concluding remarks. We have reviewed two alternatives to traditional MPC algorithms when controlling large-scale interacting particle systems. Firstly, we have shown that the use of supervised learning techniques in conjunction with deep neural networks is a suitable method for building a suboptimal feedback law based on a finite number of offline samples from optimal trajectories. Synthetic optimal trajectory generation can be

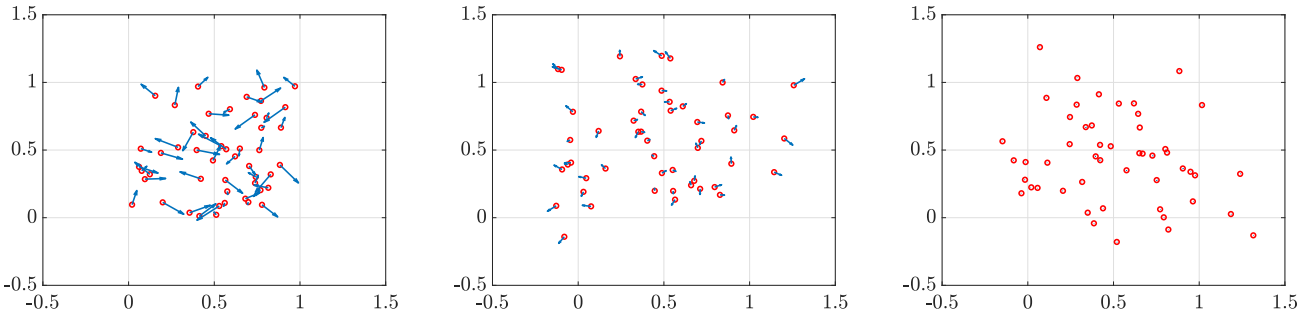


Figure 4: **Test 2:** System configuration at time $t = 0, 1, 10$ seconds respectively, under the control action provided by \mathbf{u}^{MdPC} with tolerance $\delta_{tol} = 0.1$.

$\mathbf{u}^{MdPC} (\delta_{tol} = 1)$	$\mathbf{u}^{MdPC} (\delta_{tol} = 0.1)$
0.221	0.227

Table 3: **Test 2:** CPU time (in seconds) required for the system integration along time $t \in [0, 10]$ under the MdPC approach for different tolerances δ_{tol} .

done either using first-order optimality conditions in Pontryagin form or by following a State-dependent Riccati Equation approach. In both cases, the high-dimensional control system makes online computation prohibitively expensive, but can be addressed in an offline training phase. Secondly, we propose a moment-driven predictive control framework, where fast online feedback synthesis is achieved by linearization, which is re-computed based on macroscopic quantities of the particle system. This method is suboptimal when compared to nonlinear control laws, but provides a fast computable alternative which do not rely on offline training of a feedback law.

References

- [1] G. Albi, N. Bellomo, L. Fermo, S.-Y. Ha, J. Kim, L. Pareschi, D. Poyato, and J. Soler. Vehicular traffic, crowds, and swarms: from kinetic theory and multiscale methods to applications and research perspectives. *Math. Models Methods Appl. Sci.*, 29(10):1901–2005, 2019.
- [2] G. Albi, S. Bicego, and D. Kalise. Gradient-augmented supervised learning of optimal feedback laws using state-dependent Riccati equations. *IEEE Control Systems Letters*, 6:836–841, 2021.
- [3] G. Albi, S. Bicego, and D. Kalise. Supervised learning for kinetic consensus control. *IFAC-PapersOnLine*, 55(30):103–108, 2022.
- [4] G. Albi, M. Bongini, E. Cristiani, and D. Kalise. Invisible control of self-organizing agents leaving unknown environments. *SIAM J. Appl. Math.*, 76(4):1683–1710, 2016.
- [5] G. Albi, E. Calzola, and G. Dimarco. A data-driven kinetic model for opinion dynamics with social network contacts. *preprint arXiv 2307.00906*, 2023.
- [6] G. Albi, Y.-P. Choi, M. Fornasier, and D. Kalise. Mean field control hierarchy. *Appl. Math. Optim.*, 76(1):93–135, 2017.
- [7] G. Albi, M. Herty, D. Kalise, and C. Segala. Moment-driven predictive control of mean-field collective dynamics. *SIAM Journal on Control and Optimization*, 60(2):814–841, 2022.
- [8] G. Albi, L. Pareschi, and M. Zanella. Boltzmann-type control of opinion consensus through leaders. *Philos. Trans. R. Soc. Lond. Ser. A Math. Phys. Eng. Sci.*, 372(2028):20140138, 18, 2014.
- [9] A. Alessio and A. Bemporad. A survey on explicit model predictive control. *Nonlinear Model Predictive Control: Towards New Challenging Applications*, pages 345–369, 2009.

[10] A. Alla, D. Kalise, and V. Simoncini. State-dependent riccati equation feedback stabilization for nonlinear pdes. *Advances in Computational Mathematics*, 49:1–32, 2021.

[11] N. Altmüller and L. Grüne. Distributed and boundary model predictive control for the heat equation. *GAMM-Mitteilungen*, 35(2):131–145, 2012.

[12] B. Azmi, D. Kalise, and K. Kunisch. Optimal feedback law recovery by gradient-augmented sparse polynomial regression. *Journal of Machine Learning Research*, 22(48):1–32, 2021.

[13] R. Bailo, M. Bongini, J. A. Carrillo, and D. Kalise. Optimal consensus control of the Cucker-Smale model. *IFAC-PapersOnLine*, 51(13):1–6, 2018.

[14] H. T. Banks, B. M. Lewis, and H. T. Tran. Nonlinear feedback controllers and compensators: a state-dependent riccati equation approach. *Computational Optimization and Applications*, 37:177–218, 2007.

[15] M. Bardi, I. C. Dolcetta, et al. *Optimal control and viscosity solutions of Hamilton-Jacobi-Bellman equations, Section 3.4*, volume 12. Springer, 1997.

[16] E. N. Barron and R. Jensen. The pontryagin maximum principle from dynamic programming and viscosity solutions to first-order partial differential equations. *Transactions of the American Mathematical Society*, 298(2):635–641, 1986.

[17] N. Bellomo and J. Soler. On the mathematical theory of the dynamics of swarms viewed as complex systems. *Math. Models Methods Appl. Sci.*, 22(suppl. 1):1140006, 29, 2012.

[18] A. Bemporad, M. Morari, V. Dua, and E. N. Pistikopoulos. The explicit linear quadratic regulator for constrained systems. *Automatica*, 38(1):3–20, 2002.

[19] J. Berberich, J. Köhler, M. A. Müller, and F. Allgöwer. Linear tracking MPC for nonlinear systems—part i: The model-based case. *IEEE Transactions on Automatic Control*, 67(9):4390–4405, 2022.

[20] V. D. Blondel, J. M. Hendrickx, and J. N. Tsitsiklis. On krause’s multi-agent consensus model with state-dependent connectivity. *IEEE transactions on Automatic Control*, 54(11):2586–2597, 2009.

[21] M. Burger, R. Pinnau, C. Totzeck, O. Tse, and A. Roth. Instantaneous control of interacting particle systems in the mean-field limit. *J. Comput. Phys.*, 405:109181, 20, 2020.

[22] J. A. Cañizo, J. A. Carrillo, and J. Rosado. A well-posedness theory in measures for some kinetic models of collective motion. *Math. Models Methods Appl. Sci.*, 21(03):515–539, 2011.

[23] P. Cannarsa and H. Frankowska. Value function, relaxation, and transversality conditions in infinite horizon optimal control. *Journal of Mathematical Analysis and Applications*, 457(2):1188–1217, 2018. Special Issue on Convex Analysis and Optimization: New Trends in Theory and Applications.

[24] M. Caponigro, M. Fornasier, B. Piccoli, and E. Trélat. Sparse stabilization and control of alignment models. *Math. Models Methods Appl. Sci.*, 25(3):521–564, 2015.

[25] J. A. Carrillo, Y.-P. Choi, and M. Hauray. The derivation of swarming models: mean-field limit and Wasserstein distances. In *Collective dynamics from bacteria to crowds*, pages 1–46. Springer, 2014.

[26] J. A. Carrillo, M. Fornasier, G. Toscani, and F. Vecil. Particle, kinetic, and hydrodynamic models of swarming. In *Mathematical modeling of collective behavior in socio-economic and life sciences*, pages 297–336. Springer, 2010.

[27] J. A. Carrillo, D. Kalise, F. Rossi, and E. Trélat. Controlling swarms toward flocks and mills. *SIAM Journal on Control and Optimization*, 60(3):1863–1891, 2022.

[28] Y.-P. Choi, D. Kalise, J. Peszek, and A. A. Peters. A collisionless singular Cucker-Smale model with decentralized formation control. *SIAM J. Appl. Dyn. Syst.*, 18(4):1954–1981, 2019.

[29] F. H. Clarke and R. B. Vinter. The relationship between the maximum principle and dynamic programming. *SIAM Journal on Control and Optimization*, 25(5):1291–1311, 1987.

[30] S. Cordier, L. Pareschi, and G. Toscani. On a kinetic model for a simple market economy. *J. Stat. Phys.*, 120(1-2):253–277, 2005.

[31] I. D. Couzin, J. Krause, N. R. Franks, and S. A. Levin. Effective leadership and decision-making in animal groups on the move. *Nature*, 433(7025):513–516, 2005.

[32] E. Cristiani, B. Piccoli, and A. Tosin. *Multiscale modeling of pedestrian dynamics*, volume 12 of *MS&A. Model. Simul. Appl.* Springer, Cham, 2014.

[33] F. Cucker and S. Smale. Emergent behavior in flocks. *IEEE Transactions on automatic control*, 52(5):852–862, 2007.

[34] F. Cucker, S. Smale, and D.-X. Zhou. Modeling language evolution. *Foundations of Computational Mathematics*, 4:315–343, 2004.

[35] P. Degond, J.-G. Liu, S. Motsch, and V. Panferov. Hydrodynamic models of self-organized dynamics: derivation and existence theory. *Methods Appl. Anal.*, 20(2):89–114, 2013.

[36] S. Dolgov, D. Kalise, and L. Saluzzi. Optimizing semilinear representations for state-dependent riccati equation-based feedback control. *IFAC-PapersOnLine*, 55(30):510–515, 2022. 25th International Symposium on Mathematical Theory of Networks and Systems MTNS 2022.

[37] S. Dolgov, D. Kalise, and L. Saluzzi. Data-driven tensor train gradient cross approximation for hamilton–jacobi–bellman equations. *SIAM Journal on Scientific Computing*, 45(5):A2153–A2184, 2023.

[38] J. R. Dyer, A. Johansson, D. Helbing, I. D. Couzin, and J. Krause. Leadership, consensus decision making and collective behaviour in humans. *Philos. Trans. Roy. Soc. B*, 364(1518):781–789, 2009.

[39] M. R. D’Orsogna, Y.-L. Chuang, A. L. Bertozzi, and L. S. Chayes. Self-propelled particles with soft-core interactions: patterns, stability, and collapse. *Phys. Rev. Lett.*, 96(10):104302, 2006.

[40] A. Eqtami, D. V. Dimarogonas, and K. J. Kyriakopoulos. Event-based model predictive control for the cooperation of distributed agents. In *2012 Amer. Control Conf.*, pages 6473–6478, 2012.

[41] G. Estrada-Rodriguez and H. Gimperlein. Interacting particles with Lévy strategies: limits of transport equations for swarm robotic systems. *SIAM J. Appl. Math.*, 80(1):476–498, 2020.

[42] M. Fornasier, S. Lisini, C. Orreri, and G. Savaré. Mean-field optimal control as gamma-limit of finite agent controls. *European J. Appl. Math.*, 30(6):1153–1186, 2019.

[43] M. Fornasier and F. Solombrino. Mean-field optimal control. *ESAIM Control Optim. Calc. Var.*, 20(4):1123–1152, 2014.

[44] G. Freudenthaler and T. Meurer. PDE-based multi-agent formation control using flatness and backstepping: analysis, design and robot experiments. *Automatica*, 115:108897, 13, 2020.

[45] J. Garnier, G. Papanicolaou, and T.-W. Yang. Consensus convergence with stochastic effects. *Vietnam J. Math.*, 45(1-2):51–75, 2017.

[46] J. Gómez-Serrano, C. Graham, and J.-Y. Le Boudec. The bounded confidence model of opinion dynamics. *Math. Models Methods Appl. Sci.*, 22(2):1150007, 46, 2012.

[47] S.-Y. Ha, T. Ha, and J.-H. Kim. Emergent behavior of a cucker-smale type particle model with nonlinear velocity couplings. *IEEE Transactions on Automatic Control*, 55(7):1679–1683, 2010.

[48] J. Hahn, U. Kruger, and T. F. Edgar. Application of model reduction for model predictive control. *IFAC Proceedings Volumes*, 35(1):393–398, 2002. 15th IFAC World Congress.

[49] Y. Han, A. Hegyi, Y. Yuan, S. Hoogendoorn, M. Papageorgiou, and C. Roncoli. Resolving freeway jam waves by discrete first-order model-based predictive control of variable speed limits. *Transportation Research Part C: Emerging Technologies*, 77:405–420, 2017.

[50] M. Herty and D. Kalise. Suboptimal nonlinear feedback control laws for collective dynamics. In *2018 IEEE 14th International Conference on Control and Automation (ICCA)*, pages 556–561. IEEE, 2018.

[51] M. Herty and L. Pareschi. Fokker-Planck asymptotics for traffic flow models. *Kinet. Relat. Models*, 3(1):165–179, 2010.

[52] M. Herty, L. Pareschi, and S. Steffensen. Mean–field control and Riccati equations. *Netw. Heterog. Media*, 10(3):699, 2015.

[53] M. Herty and C. Ringhofer. Averaged kinetic models for flows on unstructured networks. *Kinet. Relat. Models*, 4(4):1081–1096, 2011.

[54] R. Herzog and K. Kunisch. Algorithms for pde-constrained optimization. *GAMM-Mitteilungen*, 33(2):163–176, 2010.

[55] L. Hewing, K. P. Wabersich, M. Menner, and M. N. Zeilinger. Learning-based model predictive control: Toward safe learning in control. *Annual Review of Control, Robotics, and Autonomous Systems*, 3(1):269–296, 2020.

[56] S. Hovland, K. Willcox, and J. T. Gravdahl. MPC for large-scale systems via model reduction and multi-parametric quadratic programming. In *Proceedings of the 45th IEEE Conference on Decision and Control*, pages 3418–3423, 2006.

[57] M. Huang, P. E. Caines, and R. P. Malhamé. Individual and mass behaviour in large population stochastic wireless power control problems: centralized and nash equilibrium solutions. In *42nd IEEE International Conference on Decision and Control (IEEE Cat. No. 03CH37475)*, volume 1, pages 98–103. IEEE, 2003.

[58] A. Jones and A. Astolfi. On the solution of optimal control problems using parameterized state-dependent Riccati equations. In *2020 59th IEEE Conference on Decision and Control (CDC)*, pages 1098–1103, 2020.

[59] A. J. King, S. J. Portugal, D. Strömbom, R. P. Mann, J. A. Carrillo, D. Kalise, G. de Croon, H. Barnett, P. Scerri, R. Groß, D. R. Chadwick, and M. Papadopoulou. Biologically inspired herding of animal groups by robots. *Methods in Ecology and Evolution*, 14(2):478–486, 2023.

[60] D. P. Kingma and J. Ba. Adam: A method for stochastic optimization. In Y. Bengio and Y. LeCun, editors, *3rd International Conference on Learning Representations, ICLR 2015, San Diego, CA, USA, May 7-9, 2015, Conference Track Proceedings*, 2015.

[61] J. Kocijan and R. Murray-Smith. *Nonlinear Predictive Control with a Gaussian Process Model*, pages 185–200. Springer Berlin Heidelberg, Berlin, Heidelberg, 2005.

[62] J. Kocijan, R. Murray-Smith, C. Rasmussen, and B. Likar. Predictive control with gaussian process models. In *The IEEE Region 8 EUROCON 2003. Computer as a Tool.*, volume 1, pages 352–356 vol.1, 2003.

[63] S. Lale, K. Azizzadenesheli, B. Hassibi, and A. Anandkumar. Model learning predictive control in nonlinear dynamical systems. In *2021 60th IEEE Conference on Decision and Control (CDC)*, pages 757–762, 2021.

[64] D. Limon, J. Calliess, and J. Maciejowski. Learning-based nonlinear model predictive control. *IFAC-PapersOnLine*, 50(1):7769–7776, 2017. 20th IFAC World Congress.

[65] B. Lincoln and A. Rantzer. Relaxing dynamic programming. *IEEE Transactions on Automatic Control*, 51(8):1249–1260, 2006.

[66] E. Maddalena, C. da S. Moraes, G. Waltrich, and C. Jones. A neural network architecture to learn explicit MPC controllers from data. *IFAC-PapersOnLine*, 53(2):11362–11367, 2020. 21st IFAC World Congress.

[67] M. Maiworm, D. Limon, and R. Findeisen. Online learning-based model predictive control with gaussian process models and stability guarantees. *International Journal of Robust and Nonlinear Control*, 31(18):8785–8812, 2021.

[68] J. E. Morinelly and B. E. Ydstie. Dual MPC with reinforcement learning. *IFAC-PapersOnLine*, 49(7):266–271, 2016. 11th IFAC Symposium on Dynamics and Control of Process SystemsIncluding Biosystems DYCOPS-CAB 2016.

[69] S. Motsch and E. Tadmor. Heterophilious dynamics enhances consensus. *SIAM review*, 56(4):577–621, 2014.

[70] A. Norouzi, H. Heidarifar, H. Borhan, M. Shahbakti, and C. R. Koch. Integrating machine learning and model predictive control for automotive applications: A review and future directions. *Engineering Applications of Artificial Intelligence*, 120:105878, 2023.

[71] K.-K. Oh, M.-C. Park, and H.-S. Ahn. A survey of multi-agent formation control. *Automatica*, 53:424–440, 2015.

[72] A. A. Peters, R. H. Middleton, and O. Mason. Leader tracking in homogeneous vehicle platoons with broadcast delays. *Automatica*, 50(1):64–74, 2014.

[73] S. S. Pon Kumar, A. Tulisan, B. Gopaluni, and P. Loewen. A deep learning architecture for predictive control. *IFAC-PapersOnLine*, 51(18):512–517, 2018. 10th IFAC Symposium on Advanced Control of Chemical Processes ADCHEM 2018.

- [74] L. S. Pontryagin, V. G. Boltyanskii, R. V. Gamkrelidze, and E. F. Mishchenko. *The mathematical theory of optimal processes, Chapter 1*. Classics of Soviet Mathematics. Interscience Publishers John Wiley & Sons, Inc., 1962. Translated from the Russian by K. N. Trirogoff; edited by L. W. Neustadt.
- [75] R. E. Stern, S. Cui, M. L. Delle Monache, R. Bhadani, M. Bunting, M. Churchill, N. Hamilton, H. Pohlmann, F. Wu, B. Piccoli, et al. Dissipation of stop-and-go waves via control of autonomous vehicles: Field experiments. *Transp. Research Part C: Emerging Techn.*, 89:205–221, 2018.
- [76] N. Subbotina. The method of characteristics for Hamilton–Jacobi equations and applications to dynamical optimization. *Journal of mathematical sciences*, 135:2955–3091, 2006.
- [77] G. Toscani. Kinetic models of opinion formation. *Commun. Math. Sci.*, 4(3):481–496, 2006.
- [78] A. Tosin and M. Zanella. Kinetic-controlled hydrodynamics for traffic models with driver-assist vehicles. *Multiscale Model. Simul.*, 17(2):716–749, 2019.
- [79] I. J. Wolf and W. Marquardt. Fast NMPC schemes for regulatory and economic NMPC – a review. *Journal of Process Control*, 44:162–183, 2016.
- [80] T. Zhao, Y. Zheng, J. Gong, and Z. Wu. Machine learning-based reduced-order modeling and predictive control of nonlinear processes. *Chemical Engineering Research and Design*, 179:435–451, 2022.
- [81] X. Zhou. Maximum principle, dynamic programming, and their connection in deterministic control. *Journal of Optimization Theory and Applications*, 65(2):363–373, 1990.